Applied Surface Science 353 (2015) 958–963

Contents lists available at ScienceDirect

Applied Surface Science

journal homepage: www.elsevier.com/locate/apsusc

Electrical activation of nitrogen heavily implanted 3C-SiC(1 0 0)

Fan Li[a,*], Yogesh Sharma[a], Vishal Shah[a], Mike Jennings[a], Amador Pérez-Tomás[c], Maksym Myronov[b], Craig Fisher[a], David Leadley[b], Phil Mawby[a]

[a] School of Engineering, University of Warwick, Coventry CV4 7AL, United Kingdom
[b] Physics Department, University of Warwick, Coventry CV4 7AL, United Kingdom
[c] ICN2 – Institut Catala de Nanociència i Nanotecnologia, Campus UAB, 08193 Bellaterra, Barcelona, Spain

ARTICLE INFO

Article history:
Received 17 March 2015
Received in revised form 24 June 2015
Accepted 26 June 2015
Available online 10 July 2015

Keywords:
3C-SiC
Post-implantation activation
Van der Pauw
Hall
Degenerated film

ABSTRACT

A degenerated wide bandgap semiconductor is a rare system. In general, implant levels lie deeper in the band-gap and carrier freeze-out usually takes place at room temperature. Nevertheless, we have observed that heavily doped n-type degenerated 3C-SiC films are achieved by nitrogen implantation level of $\sim 6 \times 10^{20}$ cm^{-3} at 20 K. According to temperature dependent Hall measurements, nitrogen activation rates decrease with the doping level from almost 100% (1.5×10^{19} cm^{-3}, donor level 15 meV) to ~12% for 6×10^{20} cm^{-3}. Free donors are found to saturate in 3C-SiC at $\sim 7 \times 10^{19}$ cm^{-3}. The implanted film electrical performances are characterized as a function of the dopant doses and post implantation annealing (PIA) conditions by fabricating Van der Pauw structures. A deposited SiO_2 layer was used as the surface capping layer during the PIA process to study its effect on the resultant film properties. From the device design point of view, the lowest sheet resistivity (~1.4 mΩ cm) has been observed for medium doped (4×10^{19} cm^{-3}) sample with PIA 1375 °C 2 h without a SiO_2 cap.

1. Introduction

Silicon carbide (SiC) has been considered as the future power devices materials attributed to its superior electrical, mechanical and thermal properties. 3C-SiC has a smaller bandgap (2.3 eV) than 4H-SiC (3.2 eV), but still two times higher than Si (1.1 eV) and can be grown directly on large area Si substrate via chemical vapour deposition (CVD) methods [1–3]. In addition, compared with 4H-SiC, 3C-SiC has a much better interface with SiO_2 [4], thus is promising in medium voltage (0.6–1.2 kV) MOSFET applications, where channel resistance is crucial.

Highly doped regions are desired for good ohmic contact and low sheet resistance in power devices design. Due to the low diffusion coefficients of dopants in SiC, highly doped layers are mostly obtained by selective ion-implantation, and after that a high temperature (1400–1700 °C) [5] PIA process is usually applied to repair the lattice damage induced by implantation, which can otherwise degrade the semiconductor layer electrical properties [6]. A roughened surface, enhanced at implanted regions, often emerges after PIA and can deteriorate the SiC interface performance such as the Schottky contact and FET channel [7–9]. A protection capping layer is often used to preserve the SiC surface during PIA, such cap materials studied include AlN [10,11], BN/AlN [12] and graphite [8,13]. AlN and BN/AlN processes are found complex and expensive, thus not widely accepted. The graphite cap proved to be effective up to 1800 °C [14] but can reduce the MOSFET channel mobility due to the excessive silicon vacancies induced by the reaction between diffused Si atoms and the graphite [14,15]. A SiO_2 layer, which should not react with Si or C, can be easily deposited by CVD method and removed via HF etching. It was also studied and resulted a similar surface roughness level as a graphite cap [16]. For 3C-SiC on Si wafers, the PIA temperature is limited by the melting point of Si (1412 °C), well below that of SiO_2 (1610 °C) [9] so a SiO_2 capping layer can be a good choice. Previously, n-type heavily implanted 3C-SiC was studied for different annealing conditions with [17] and without [18,19] a graphite cap. A study of using deposited SiO_2 as the PIA capping layer for 3C-SiC on Si is demonstrated here. Results are reported for the implanted layer sheet resistivity, dopant activation (energy and rate) and free carrier mobility of nitrogen implanted 3C-SiC layer as following parameters: implantation doses, PIA conditions and SiO_2 capping effects.

2. Experimental procedures

The materials studied in this work was a 10 μm thick unintentionally doped (<1×10^{16} cm^{-3}) 3C-SiC film epitaxial grown on

* Corresponding author.
E-mail addresses: f.li.1@warwick.ac.uk, lithiumfantasy@gmail.com (F. Li).

http://dx.doi.org/10.1016/j.apsusc.2015.06.169
0169-4332/

Table 1
Post-implantation activation annealing conditions.

Temperature [°C]	1175	1275	1275	1375	1375
Duration [h]	2	1	2	1	2

a 4 in Si(1 0 0) substrate by NOVASiC. The wafer went through a chemical–mechanical polishing process [20] after the CVD growth with an initial surface RMS roughness ~0.2 nm determined from atomic force microscopy (AFM) measurements. A Veeco multimode AFM with Nanonis controller was used to evaluate the surface roughness. The overall roughness value was determined by scanning three 10 μm × 10 μm areas and averaging the results. The wafer was cut into 30 8 mm × 8 mm pieces and equally divided into 3 batches. An on-axis nitrogen implantation process was conducted on the plain surface of all samples at room temperature. A series of energies with increasing total doses were applied during implantation to form box profile at three doping levels, which will be called high dose, medium dose and low dose samples in following text. Nitrogen was selected as the dopant rather than phosphorous since it does less damage to the 3C-SiC film [17,18], although it saturates more readily [8]. Prior to the PIA process, 1 μm thick SiO_2 was deposited on the surface of half samples from each batch via plasma enhanced chemical vapour deposition (PECVD). To study the SiO_2 cap effect, one capped and one uncapped sample from each batch (six all together) went through the PIA process with continuous Ar flow at 5 slm. Five PIA conditions as shown in Table 1 (for each condition two samples from each batch) with different annealing temperature and time durations were applied to study PIA process effects on resultant 3C-SiC properties. The maximum annealing temperature applied was determined as 1375 °C, just below the Si substrate melting point 1412 °C [21]. The SiO_2 cap layer was removed by HF etching, after which, all samples were solvent cleaned followed by a standard RCA procedure. Van der Pauw structures were then patterned using lithography and ICP etching. A previously reported process [22] was used for the ohmic contacts formation in this work: Ti(30 nm)/Ni(80 nm) bilayer metal contacts were deposited at low pressure (2×10^{-7} mBar) in an E-beam evaporator and annealed for 1 min at 1000 °C in a rapid thermal anneal (RTA) furnace with continuous Ar flow. The Van der Pauw structures were 1 μm deep 1 mm^2 square mesas with 100 μm × 100 μm contact pads on four corners. All contacts were isolated by 1 μm deposited SiO_2 to reduce surface recombination effects. Room temperature IV measurements were made on the Van der Pauw structures to study the implanted film sheet resistivity. Temperature dependent Hall measurements were also conducted with a magnetic field strength of 800 mT and an input current of 10 μA for free carrier concentration and mobility evaluation.

3. Results and discussions

3.1. Surface roughness evolution

Fig. 1 illustrates the surface morphology change of samples from each dose batch after a 1 h PIA process at 1375 °C. It can be noticed that regardless of the dose levels, all groups experienced a surface degradation, although the high dose sample surfaces were

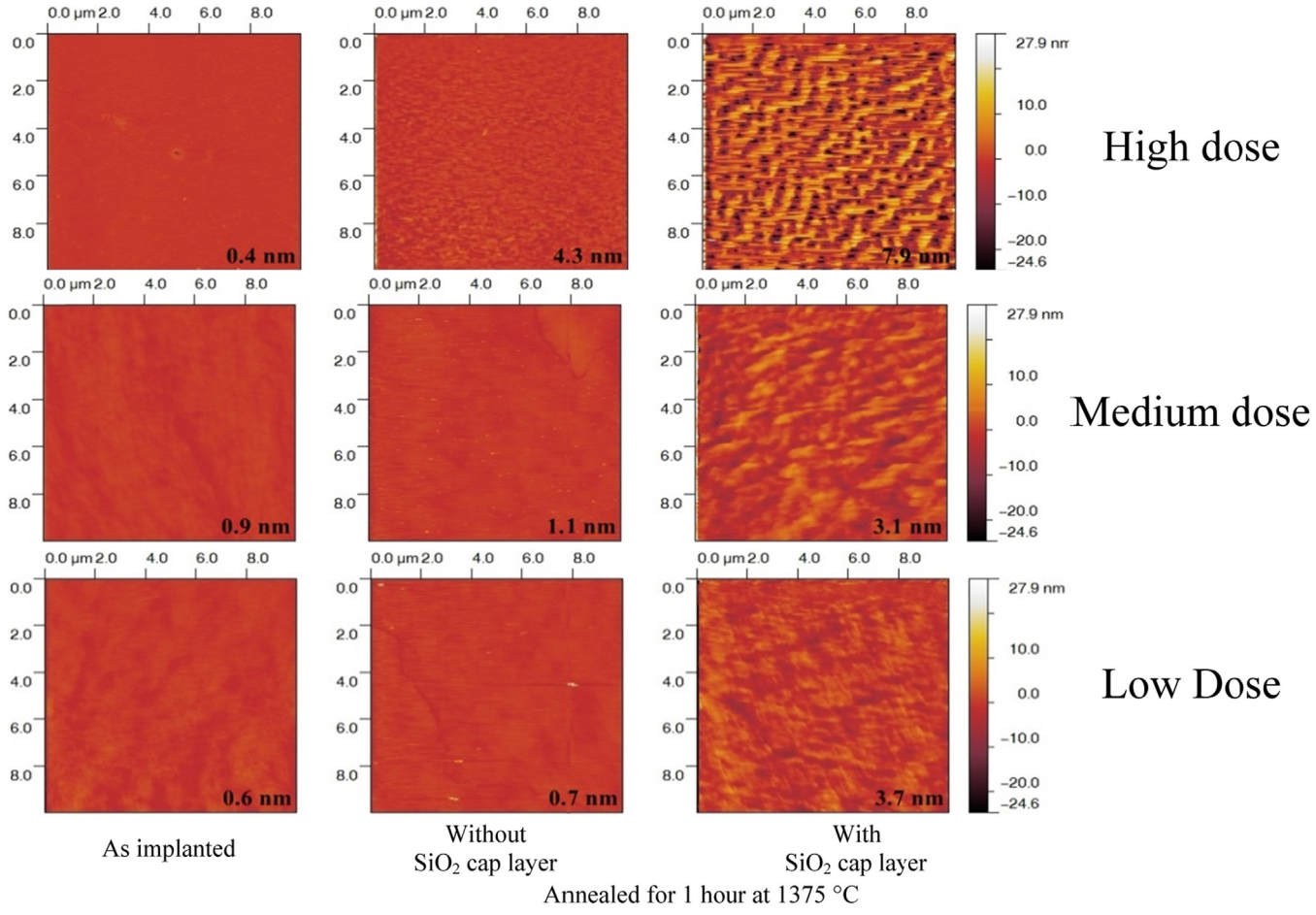

Fig. 1. AFM images of 3C-SiC surface for 3 doses, inset values are RMS surface roughness values.

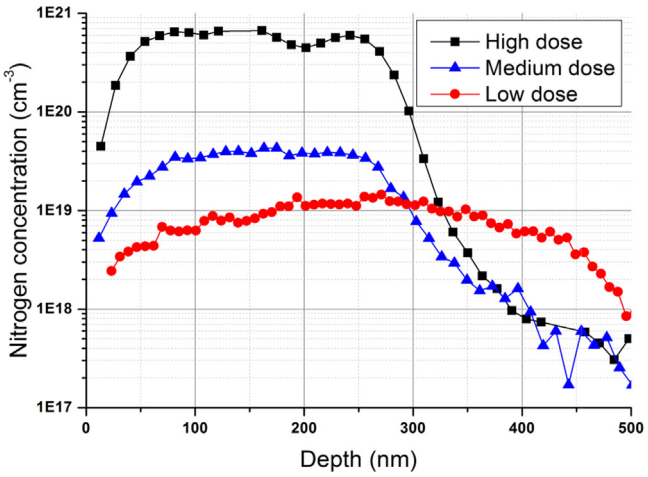

Fig. 2. SIMS profiles for 3 dose samples after post implantation annealing at 1375 °C for 2 h.

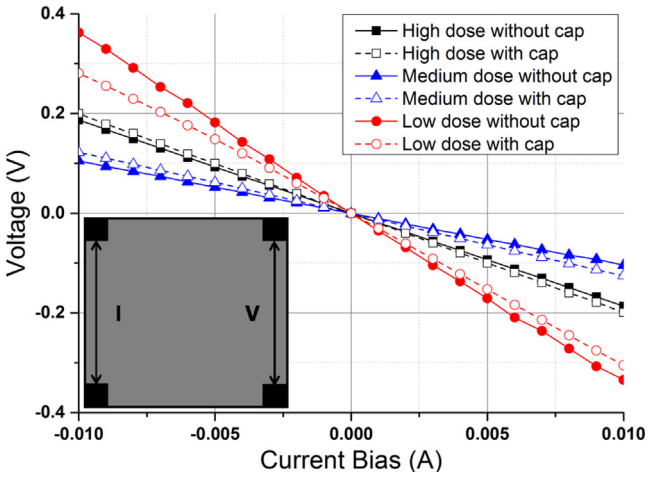

Fig. 3. Room temperature IV curves of Van der Pauw structures annealed at 1375 °C for 1 h.

degraded more severely, indicating higher lattice damage [5,18]. The SiO_2 capped samples were left with a higher roughness compared with the uncapped ones in all batches. A considerable amount of pits were observed on the SiO_2 capped high dose sample, resulting in a higher surface roughness value of 7.9 nm compared with as implanted (0.4 nm) and without a cap (4.3 nm). The SiO_2 cap aimed at protecting the 3C-SiC surface led to a worse surface morphology, conflicting with the 4H-SiC case [16]. This is probably due to the interaction between SiO_2 and SiC, which was not supposed to occur at 1400 °C but can be triggered by the high impurity concentration [23].

3.2. SIMS profiles

After the PIA process, second ion mass spectrometry (SIMS) analysis was conducted on samples from each dose batch for the toughest PIA condition (1375 °C, 2 h) as shown in Fig. 2. The profiles before PIA were not shown here but were expected to be much like the annealed ones due to the unlikely observable diffusion of nitrogen in 3C-SiC below 1800 °C [17,24]. High dose and medium dose samples both achieved an implantation depth of ~300 nm with peak values around 6×10^{20} and 4×10^{19} cm^{-3}, respectively. For the low dose sample, a depth of ~500 nm was observed and the peak doping value was determined as around 1.5×10^{19} cm^{-3}.

3.3. Room temperature IV measurements

IV measurements were conducted on the fabricated Van der Pauw structures at room temperature. Linear IV curves were obtained for all samples (see Fig. 3), indicating a typical ohmic behaviour for the Ti/Ni bilayer metal contacts. Sheet resistivity values can be calculated following Eq. (1) [25], where t is the film thickness and R is the resistance value obtained from IV measurements using the configurations shown in Fig. 3.

$$\rho = \frac{\pi}{\ln(2)} tR \tag{1}$$

Due to the existence of a conduction n-type epilayer (see Fig. 4), the resistance R can be considered as the result of paralleling the implantation and epilayer layer resistance and the implanted layer sheet resistivity $\rho_{sh,imp}$ can be calculated following Eqs. (2)–(4), where T is the as grown epilayer thickness, t is the implanted film thickness, q is the electron charge, $N_{D,epi}$ is the epilayer doping

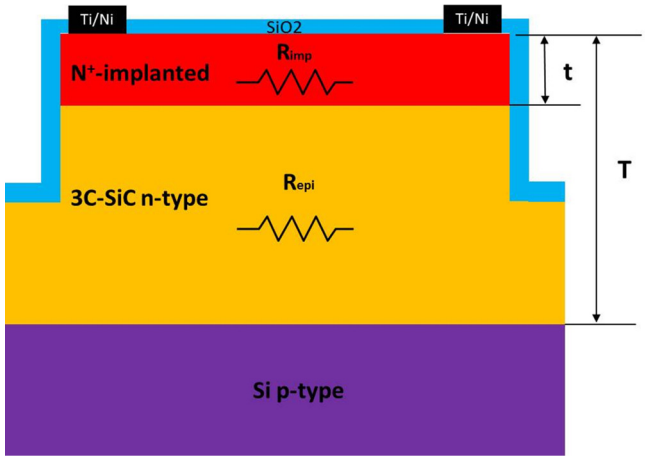

Fig. 4. The implanted layer sheet resistivity calculation model.

1×10^{16} cm^{-3} and μ_{epi} is the epilayer electron mobility 763 $cm^2/V\,s$ [26].

$$\frac{1}{R} \approx \frac{1}{R_{imp}} + \frac{1}{R_{epi}} \tag{2}$$

$$R_{epi} = \left(\frac{\ln 2}{\pi}\right)\left(\frac{1}{T-t}\right)\rho_{sh,epi} = \left(\frac{\ln 2}{\pi}\right)\left(\frac{1}{T-t}\right)\frac{1}{qN_{D,epi}\mu_{epi}} \tag{3}$$

$$\rho_{sh,imp} = \frac{\pi}{\ln(2)} tR_{imp} = \frac{\pi}{\ln(2)} t\left(\frac{RR_{epi}}{R_{epi}-R}\right) \tag{4}$$

The resultant sheet resistivity values are plotted as a function of annealing conditions in Fig. 5. It can be seen that for the medium dose sample, sheet resistivity values for capped and uncapped samples both gradually decrease with PIA process temperature and time durations. The lowest sheet resistivity value is ~1.4 mΩ cm obtained for the 2 h 1375 °C annealing condition. There is more than 50% reduction comparing with the 2 h 1175 °C process. This observed trend suggests an increasing nitrogen activation rate accomplished by raising annealing temperature as well as time durations. The SiO_2 capped samples for medium dose case all yielded a slightly higher sheet resistivity value. Relating this to the mild surface roughening observed on the SiO_2 capped sample compared with the uncapped one (2 nm difference in Fig. 1), it suggests that for a doping level of ~4×10^{19} cm^{-3}, surface roughness is an important indicator for evaluating implanted film electrical performance. For the high dose sample, the dependence of sheet

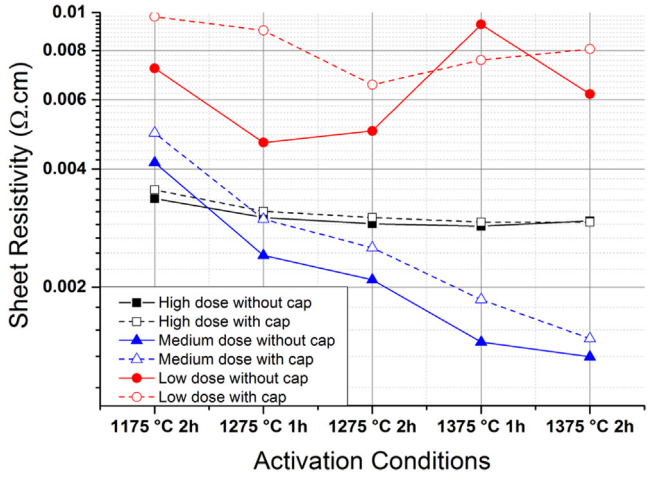

Fig. 5. Effect of activation temperatures and time durations on implanted layer sheet resistivity.

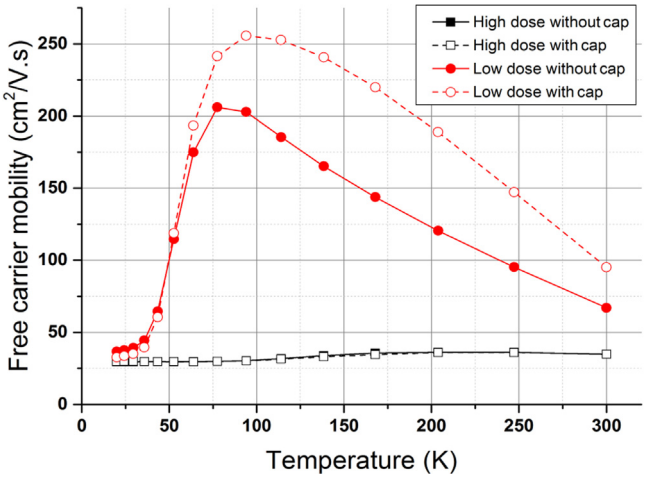

Fig. 6. Temperature dependence of implanted 3C-SiC film electron mobility for high and low doses.

resistivity on annealing conditions is much weaker that can be barely determined. This is most likely caused by the saturation of free donors in 3C-SiC [27], which means a higher concentration of active N donors is physically impossible even with higher annealing temperatures or longer time periods. There is almost no difference between capped and uncapped samples in high dose case, even with a bigger surface roughness difference (3.6 nm difference) and much more obvious surface morphology change (pits formation for SiO_2 capped sample). This indicates that in this high doping level (6×10^{20} cm^{-3}), surface roughness influence is negligible. The low dose samples, however, demonstrate quite random sheet resistivity behaviour. A possible explanation is that in this case, all nitrogen dopants have been activated and the fluctuations in the sheet resistivity curve actually come from the disturbance of contact resistance, which is known to be heavily dependent on the semiconductor doping level [5]. It was later found out the low dose sample contact resistance was one order of magnitude higher than the high dose and medium dose ones (not shown here). The Hall measurements results are also in favour of this assumption.

3.4. Temperature dependent Hall measurements

Low temperature Hall measurements were made on the high dose and low dose sample annealed at 1375 °C for 1 h. The studied temperature range was between 20 and 300 K and Fig. 6 is the temperature dependent free carrier mobility curve. Due to a high impurity scattering effect, the high dose curve shows almost no temperature dependence. In low dose case, peak mobility value around 250 cm^2/V s is achieved at 100 K for the uncapped sample and ~95 cm^2/V s at room temperature. Compared with the literature mobility results summarized in Table 2, the values obtained in this work are in agreement with the general rule that higher impurity concentration results in reduced carrier mobility. Above 100 K, free carrier mobility is dominated by phonon scattering so falls with increasing temperature roughly as $T^{-0.8}$, which is slower compared with the results obtained from more lowly doped epitaxial 3C-SiC layers, ~$T^{-1.8}$ in Ref. [28] and ~$T^{-1.2\text{–}1.4}$ in Ref. [29]. On the other hand, below 100 K, free carrier mobility drops quickly with decreasing temperature. It is probably induced by the hopping phenomenon, which means a change of the carrier transport process from free electrons to quantum mechanical tunnelling of electrons between dopant atoms. It was previously found on heavily doped n-type and p-type 4H-SiC layers when temperature was so low that free carriers were frozen on the dopants [30,31]. From the almost perfectly overlapped curves for high dose sample (in

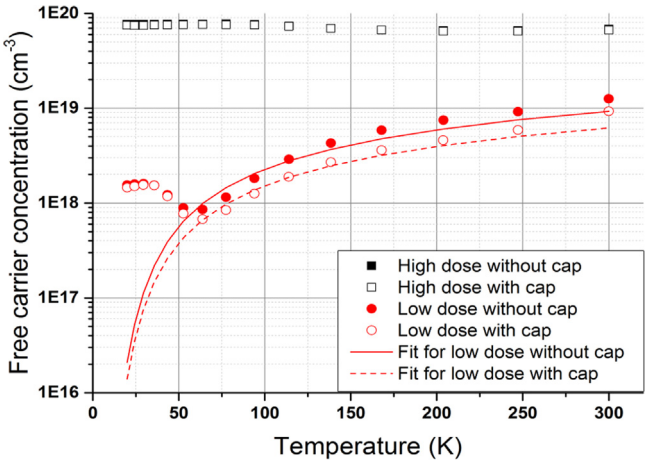

Fig. 7. Temperature dependence of implanted 3C-SiC free carrier concentration for high and low doses. (For interpretation of the references to color in text, the reader is referred to the web version of this article.)

Figs. 6–8), again it is confirmed that the SiO_2 cap has a negligible effect on high dose film electrical performance. While for the low dose sample, a considerable higher mobility is consistently observed in whole temperature range for the SiO_2 capped sample. This can be explained by a lower free carrier concentration, namely lower impurity scattering, found in the capped sample as seen in Fig. 7. For N^+ implantation on n-type epilayer in this case, the following assumptions can be made: $N_d - N_a \approx N_d$ and $1 + \alpha N_a \ll 4\alpha N_d$ with α defined in Ref. [32]. Then the temperature dependent semiconductor free carrier concentration $n(T)$ can be approximated as below:

$$n(T) = \frac{2(N_d - N_a)}{1 + \alpha N_a + \sqrt{(1 + \alpha N_a)^2 + 4\alpha(N_d - N_a)}} \approx \sqrt{(N_C/2)N_D}e^{-(E_d/2kT)} \quad (5)$$

where N_D is the free donor concentration, E_d is the dopant activation energy, k is the Boltzmann constant, T is the measuring temperature and N_C is the effective density of states in conduction band, which is further defined as:

$$N_c = 2(2\pi m_{d,e} kT/h^2)^{3/2} \quad (6)$$

where $m_{d,e}$ is the 3C-SiC effective mass of density of states ($0.72m_0$) and h is the plank constant.

Table 2
Comparison between results obtained in this work and previous literatures on n-type 3C-SiC(1 0 0), RT is room temperature.

Free carrier concentration (cm^{-3})	Growing method	PIA process	Donor activation energy (meV)	RT electron mobility ($cm^2/V\,s$)	Reference
Not given (NID)	Solution	None	53 (luminescence)	Not given	[34]
$1–3 \times 10^{16}$ (NID)	CVD on Si	None	20 (Hall)	763	[26]
$\sim 2 \times 10^{16}$ (NID)	CVD on Si	None	38 (ECR)	300	[35]
$3–7 \times 10^{16}$ (NID)	CVD on Si	None	18 (Hall)	400–550	[28]
1.2×10^{17} (NID)	CVD on Si	None	47 (Hall)	305	[33]
$0.5–1 \times 10^{18}$ (NID)	CVD on Si	None	40–50 (Hall)	120–200	[29]
$\sim 1 \times 10^{19}$ ($RT\ 1.5 \times 10^{19}\ cm^{-3}$ nitrogen implanted)	CVD on Si and implanted	1375 °C 1 h with SiO_2 cap	15 (Hall)	95	This work
$\sim 1.5 \times 10^{19}$ ($RT\ 1.5 \times 10^{19}\ cm^{-3}$ nitrogen implanted)	CVD on Si and implanted	1375 °C 1 h without cap	15 (Hall)	70	This work
$\sim 7 \times 10^{19}$ ($RT\ 6 \times 10^{20}\ cm^{-3}$ nitrogen implanted)	CVD on Si and implanted	1375 °C 1 h with/without SiO_2 cap	Degenerated	35	This work

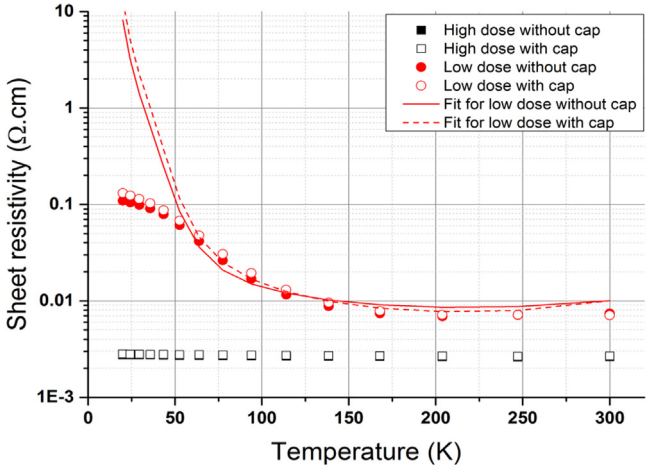

Fig. 8. Temperature dependence of implanted 3C-SiC sheet resistivity for high and low doses. (For interpretation of the references to color in text, the reader is referred to the web version of this article.)

Using N_D and E_d as fitting parameters, best theoretical fits (red solid and dashed lines in Figs. 7 and 8) were achieved with $N_D \approx 1 \times 10^{19}\,cm^{-3}$ and $\approx 1.5 \times 10^{19}\,cm^{-3}$ for capped and uncapped low dose samples respectively, with activation energy of $E_d \approx 15$ meV. Comparing with the SIMS profile in Fig. 2, an N_D value of $1.5 \times 10^{19}\,cm^{-3}$ indicates almost 100% activation for low dose uncapped case, while the SiO_2 capped sample yields a lower activation rate (≈67%). Previous results on the residual donor activation energy of 3C-SiC covered quite a range from 18 to 54 meV using various characterizing tools as shown in Table 2. 15 meV is lower than most of the literature values, but this is the first time that such a value ever reported for 3C-SiC epilayer with an implantation level $>1 \times 10^{19}\,cm^{-3}$. In Ref. [33] an expression was derived to show that the residual donor energy E_d in 3C-SiC decreased with the donor (nitrogen) concentration, and when N_d was around $1 \times 10^{19}\,cm^{-3}$, E_d approached 0, which is similar to our case. For the high dose case, a theoretical fit is impossible indicating the degeneracy of the implanted layer. And the flat out free carrier concentration values ($\sim 7 \times 10^{19}\,cm^{-3}$, 12% activation rate) in the whole temperature range for the high dose sample confirms the donor saturation in 3C-SiC. The temperature dependent sheet resistivity curves (see Fig. 8) were also obtained for high and low dose samples from Hall measurements. In Fig. 8, even for the low dose sample, sheet resistivity starts to become temperature independent above 150 K, which could mean all nitrogen donors have been thermally ionized by 150 K. For both the free carrier concentration and sheet resistivity curves, the experimental data departs from the theoretical fit below 75 K, which as mentioned before, is induced by hopping phenomenon [28]. A summary of the obtained results in this work are listed in Table 2 together with some literature results for comparison.

4. Conclusions

The dependence of the nitrogen implanted 3C-SiC layer electrical performance on the implantation doses, surface preparations and annealing conditions are investigated in this work. The surface morphology turns out to be an important indicator for low and medium doses layer properties, while not for the high dose layer. Nitrogen activation rate is found to be increasing with PIA process temperature and time durations in medium dose case. For the low and high dose samples, activation rates are not much PIA process dependent. This is due to 100% activation for low dose sample and only 12% activation rate but with donor saturation for high dose case, both confirmed by Hall measurements. By fitting the low dose sample experimental data points with a theoretical curve, an activation energy value of ∼15 meV was extracted for nitrogen in 3C-SiC. The high dose film is found be completely degenerated. Also, it was found that nitrogen donors in 3C-SiC are probably fully thermally ionized at 150 K. The results we obtained can be very useful for fabricating structures on heavily implanted 3C-SiC layers, which is very important during power devices manufacturing.

Acknowledgements

The authors would like to acknowledge the Engineering and Physical Sciences Research Council (EPSRC) for supporting the Vehicle Electrical Systems Integration (VESI) project (EP/I038543/1) and Creating Silicon Based Platforms for New Technologies project (EP/J001074/1). ICN2 acknowledges support of the Spanish MINECO through the Severo Ochoa Centers of Excellence Program under Grant SEV-2013-0295.

References

[1] A. Severino, C. Locke, F. La Via, S.E. Saddow, (Invited) high quality 3C-SiC for MOS applications, ECS Trans. 41 (2011) 273–282.
[2] N. Hatta, T. Kawahara, K. Yagi, H. Nagasawa, S.A. Reshanov, A. Schöner, Reliable method for eliminating stacking fault on 3C-SiC (0 0 1), Mater. Sci. Forum (2012) 173–176.
[3] M.R. Jennings, A. Pérez-Tomás, A. Bashir, A. Sanchez, A. Severino, P.J. Ward, et al., Bow free 4″ diameter 3C-SiC epilayers formed upon wafer-bonded Si/SiC substrates, ECS Solid State Lett. 1 (2012) P85–P88.
[4] M. Bakowski, A. Schöner, P. Ericsson, H. Strömberg, H. Nagasawa, M. Abe, Development of 3C-SiC MOSFETs, J. Telecommun. Inf. Technol. 2 (2007).
[5] M. Li, A.C. Ahyi, X. Zhu, Z. Chen, T. Isaacs-Smith, J.R. Williams, et al., Nickel Ohmic contacts to N-implanted (0 0 0 1) 4H-SiC, J. Electron. Mater. 39 (2010) 540–544.
[6] K.S. Jones, G.A. Rozgonyi, Rapid Thermal Processing: Science and Technology, Academic Press, Orlando, 1993.

[7] M.A. Capano, S. Ryu, J.A. Cooper Jr., M.R. Melloch, K. Rottner, S. Karlsson, et al., Surface roughening in ion implanted 4H-silicon carbide, J. Electron. Mater. 28 (1999) 214–218.
[8] Y. Negoro, K. Katsumoto, T. Kimoto, H. Matsunami, Electronic behaviors of high-dose phosphorus-ion implanted 4H–SiC (0 0 0 1), J. Appl. Phys. 96 (2004) 224–228.
[9] K. Vassilevski, N. Wright, I. Nikitina, A. Horsfall, A. O'Neil, M. Uren, K. Hilton, A. Masterton, A. Hydes, C. Johnson, Protection of selectively implanted and patterned silicon carbide surfaces with graphite capping layer during post-implantation annealing, Semicond. Sci. Technol. 20 (2005) 271.
[10] M.A. Derenge, K.A. Jones, K. Kirchner, M. Ervin, A comparison of the AlN annealing cap for 4H SiC annealed in a nitrogen versus an argon atmosphere, in: Semiconductor Device Research Symposium, 2003 International, 2003, pp. 126–127.
[11] K.A. Jones, P.B. Shah, K.W. Kirchner, R.T. Lareau, M.C. Wood, M.H. Ervin, et al., Annealing ion implanted SiC with an AlN cap, Mater. Sci. Eng. B 61–62 (1999) 281–286.
[12] L. Ruppalt, S. Stafford, D. Yuan, R. Vispute, T. Venkatesan, R. Sharma, et al., Using a PLD BN/AlN composite as an annealing cap for ion implanted SiC, in: Semiconductor Device Research Symposium, 2001 International, 2001, pp. 529–530.
[13] A. Frazzetto, F. Giannazzo, R.L. Nigro, V. Raineri, F. Roccaforte, Structural and transport properties in alloyed Ti/Al Ohmic contacts formed on p-type Al-implanted 4H-SiC annealed at high temperature, J. Phys. D: Appl. Phys. 44 (2011) 255302.
[14] K.A. Jones, M.C. Wood, T.S. Zheleva, K.W. Kirchner, M.A. Derenge, A. Bolonikov, et al., Structural and chemical comparison of graphite and BN/AlN caps used for annealing ion implanted SiC, J. Electron. Mater. 37 (2008) 917–924.
[15] H. Naik, K. Tang, T.P. Chow, Effect of graphite cap for implant activation on inversion channel mobility in 4H-SiC MOSFETs, in: Presented at the 7th European Conference on Silicon Carbide and Related Materials, 2009.
[16] F. Zhao, M.M. Islam, C.-F. Huang, Study of SiO_2 encapsulation for aluminum and phosphorus implant activation in 4H-SiC, Mater. Lett. 64 (2010) 2593–2596.
[17] X. Song, J. Biscarrat, J.-F. Michaud, F. Cayrel, M. Zielinski, T. Chassagne, et al., Structural and electrical characterizations of n-type implanted layers and ohmic contacts on 3C-SiC, Nucl. Instrum. Methods Phys. Res. Sect. B: Beam Interact. Mater. Atoms 269 (2011) 2020–2025.
[18] A. Bazin, J. Michaud, C. Autret-Lambert, F. Cayrel, T. Chassagne, M. Portail, et al., Ti–Ni ohmic contacts on 3C–SiC doped by nitrogen or phosphorus implantation, Mater. Sci. Eng. B 171 (2010) 120–126.
[19] T. Chassagne, D. Alquier, F. Cayrel, E. Collard, M. Portail, A.E. Bazin, et al., Electrical characterization of nitrogen implanted 3C-SiC by SSRM and CTLM measurements, Mater. Sci. Forum (2011) 193–196.
[20] H. Mank, C. Moisson, D. Turover, M.E. Twigg, S.E. Saddow, Regrowth of 3C-SiC on CMP treated 3C-SiC/Si epitaxial layers, Mater. Sci. Forum (2005) 197–200.
[21] G.L. Pearson, R.G. Treuting, Surface melt patterns on silicon, Acta Crystallogr. 11 (1958) 397–399.
[22] C.A. Fisher, M.R. Jennings, Y.K. Sharma, D.P. Hamilton, P.M. Gammon, A. Perez-Tomas, et al., Improved performance of 4H-SiC PiN diodes using a novel combined high temperature oxidation and annealing process, Semicond. Manuf. IEEE Trans. 27 (2014) 443–451.
[23] A.L. Yurkov, B.I. Polyak, Contact phenomena and interactions in the system SiC-SiO_2-R x O y in condensed matter, J. Mater. Sci. 30 (1995) 4469–4478.
[24] E. Taguchi, Y. Suzuki, M. Satoh, Electrical properties of N ion implanted layer in 3C-SiC (1 0 0) grown on self-standing 3C-SiC substrate, Mater. Sci. Forum (2007) 579–582.
[25] D.K. Schroder, Semiconductor Material and Device Characterization, John Wiley & Sons, 2006.
[26] M. Shinohara, M. Yamanaka, H. Daimon, E. Sakuma, H. Okumura, S. Misawa, K. Endo, S. Yoshida, Growth of high-mobility 3C-SiC epilayers by chemical vapor deposition, Jpn. J. Appl. Phys. 27 (1988) L434.
[27] X. Song, J. Biscarrat, A.E. Bazin, J.F. Michaud, F. Cayrel, M. Zielinski, et al., Dose influence on physical and electrical properties of nitrogen implantation in 3C-SiC on Si, Mater. Sci. Forum (2012) 154–158.
[28] M. Yamanaka, H. Daimon, E. Sakuma, S. Misawa, K. Endo, S. Yoshida, Temperature dependence of electrical properties of nitrogen-doped 3C-SiC, Jpn. J. Appl. Phys. 26 (1987) L533.
[29] K. Sasaki, E. Sakuma, S. Misawa, S. Yoshida, S. Gonda, High-temperature electrical properties of 3C-SiC epitaxial layers grown by chemical vapor deposition", Appl. Phys. Lett. 45 (1984) 72–73.
[30] N.S. Saks, A.V. Suvorov, D.C. Capell, High temperature high-dose implantation of aluminum in 4H-SiC, Appl. Phys. Lett. 84 (2004) 5195–5197.
[31] W.C. Mitchel, A.O. Evwaeaye, S.R. Smith, M.D. Roth, Hopping conduction in heavily doped bulk n-type SiC, J. Electron. Mater. 26 (1997) 113–118.
[32] A. Pérez-Tomás, A. Fontserè, M. Placidi, M.R. Jennings, P.M. Gammon, Modelling the metal–semiconductor band structure in implanted ohmic contacts to GaN and SiC, Modell. Simul. Mater. Sci. Eng. 21 (2013) 035004.
[33] B. Segall, S.A. Alterovitz, E.J. Haugland, L.G. Matus, Compensation in epitaxial cubic SiC films, Appl. Phys. Lett. 49 (1986) 584–586.
[34] P.J. Dean, W.J. Choyke, L. Patrick, The location and shape of the conduction band minima in cubic silicon carbide, J. Lumin. 15 (1977) 299–314.
[35] R. Kaplan, R.J. Wagner, H.J. Kim, R.F. Davis, Electron cyclotron resonance in cubic SiC, Solid State Commun. 55 (1985) 67–69.